

## **Applicability of fatigue solutions to floating wind turbine structures**

**Y. Kayamori, T. Inoue**

Steel Research Laboratories, Nippon Steel & Sumitomo Metal Corporation

**T. Okawa**

Oita R&D Laboratory, Nippon Steel & Sumitomo Metal Corporation

**S. Nishimura**

Plate Div., Nippon Steel & Sumitomo Metal Corporation

**T. Ishihara**

Department of Civil Engineering, The University of Tokyo

*Abstract* - Fukushima floating offshore wind farm demonstration project has started since 2012, and various subjects in floating offshore wind turbine technologies have been discussed by Fukushima floating offshore consortium in the project. The fatigue of floating wind turbine structures is one of the subjects because variable loading by external forces such as ocean winds and sea waves can lead to fatigue, and two solutions to the fatigue were investigated in this study.

One solution is ultrasonic impact treatment, UIT, and the effect of UIT on the fatigue properties of large-scale welded models was examined by using the 2.5MN large fatigue test machine. YP460 TMCP steel plates were used for manufacturing the large-scale structural models, and UIT significantly improved fatigue life particularly in the low stress range and long fatigue life region.

The other solution is steel for plasma arc cutting, which is used for a process of fabricating large-scale welded structures such as wind turbines. Notched fatigue specimens were sampled by using plasma arc cutting from two kinds of TMCP steel plates, YP460 and KD36, and their fatigue properties were investigated. In each TMCP steel plate, fatigue strength was not degraded on the plasma arc cut surface.

### I. INTRODUCTION

The Great East Japan Earthquake struck the northeastern area of Honshu in 2011, and many local industries were damaged by the earthquake and tsunami. A clue to an industrial recovery from the damage is potentially new industrial development that creates new employment in the area. After the post-tsunami shutdown and catastrophic damage of Fukushima Daiichi nuclear power plant, a possible industry is renewable energy. The Agency for Natural Resources and Energy, ANRE, in the Ministry of Economy, Trade and Industry in Japan, METI, organized Fukushima Floating Offshore Consortium, and Fukushima Floating Offshore Wind Farm Demonstration Project, Fukushima FOWARD, was launched in 2012 [1]. The aim of this project is to establish a business model of

floating large offshore wind farms. This project plans to develop three floating wind turbines and one floating power sub-station off the coast of Fukushima, and various subjects in floating offshore wind turbine technologies have been discussed by the 11-entry consortium.

Fatigue is one of the subjects because variable loading by external forces such as ocean winds and sea waves can lead to the fatigue of floating wind turbine structures. Another one is weight reduction for constructing a lot of large offshore wind turbines efficiently, and materials with high strength can contribute to weight reduction. However, the fatigue strength of steel welded joints is independent of the static tensile strength of the steel because of tensile residual stress, high stress concentration and microstructure change. Fatigue solutions are useful technologies for the improvement of fatigue strength in steel welded structures, where it is expected that the use of high tensile strength steel plates will result in high fatigue strength.

Post weld toe shape improvement methods such as burr grinding and TIG dressing are conventional fatigue solutions, and have been used for welded structures. Peening is another solution, and its effect on fatigue is higher than that of toe shape improvement only because peening induces compressive residual stress as well as smooth toe shape. Ultrasonic impact treatment, UIT, is a kind of peening methods, and has advantages in treatment speed, vibration, noise, etc. UIT also gives a good fatigue performance in welded joints [2-3], and the details of a fatigue property improvement have been investigated in recent years [4-6]. However, UIT has not applied to floating wind turbine structures, and it is unclear whether UIT improves the fatigue strength of welded joints in floating wind turbines. In this study, the effect of UIT on the fatigue properties of welded large-scale structural models, which simulated a welded connection of a tower to a floating body, was examined by using the 2.5MN large fatigue test machine. High strength YP460 steel plates were used for manufacturing the large-scale structural models.

In addition to the welded joints, base metal plates should have high fatigue strength in case the plates are used for machined and worked structural members. In a

process of fabricating large-scale welded structures such as wind turbines, the plates are often cut by plasma arc cutting machines, where the fatigue strength of a quenched and hardened cut surface is probably affected by the chemical composition of steel [7]. Accordingly, another fatigue solution is steel for plasma arc cutting, and the thermomechanical control process, TMCP, is available for making the steel. In this study, two kinds of TMCP steel plates, YP460 and KD36, were used for notched plasma arc cut specimens, and their fatigue properties were investigated.

## II. EXPERIMENTAL AND ANALYTICAL METHODS

### A. Materials

Two kinds of high strength steel plates were used for fatigue tests in this study. One was YP460, whose specified minimum yield stress, SMYS, was 460MPa, and the other was KD36, which was based on the rolled steel plates for shipbuilding ruled by the Japan ship classification society, ClassNK, and its SMYS was 355MPa. Both steel plates were manufactured by TMCP. Tables 1 and 2 show the chemical compositions and mechanical properties of the plates. YP460 was used for large-scale structural fatigue specimens, whose plate thicknesses were 25mm and 50mm, while two kinds of steel plates, YP460 and KD36, were used for notched plasma arc cut specimens, which had the identical plate thickness of 25mm.

### B. Structural Model Fatigue Tests

Fig. 1 shows a schematic floating wind turbine and a large-scale structural fatigue specimen. Most of floating wind turbine structures have brackets between a tower and a floating body, and a bracket end was selected as the location of fatigue crack initiation in the specimen. The loading type of the specimen was four point bending, and the total length of the specimen was 5,500mm. Flux cored arc welding, FCAW, was performed with wires of SF-60 (JIS Z3313 T59J1T1-1CA-N2M1- UH5, AWS A5.29 E81T1-G) using CO<sub>2</sub> as the shielding gas. The number of passes was three, and the leg length was about 15mm. Four large-scale structural specimens were manufactured; two were examined for welds with UIT, and the others were for as-welded toes for comparison. As UIT equipment,

Esonics<sup>TM</sup> 27 UIS made by Applied Ultrasonics was used in this study. The operating frequency of an ultrasonic generator was 27kHz, and the diameter of an indenter pin was 3mm in the equipment. The weld toes of the UIT specimens were treated until the original weld toes disappeared, and the maximum indent depth was about 0.4mm after the treatment, as shown in Fig. 2. Residual stress distributions near the toe and UIT lines were measured in the specimen longitudinal direction by an X-ray stress analyzer, Xstress 3000, using the X-ray diffraction ( $\sin^2\psi$ ) method, where the collimator size was set at 3mm. Compressive residual stress was dominant near the UIT lines although tensile residual stress was spread near the as-welded toe, as shown in Fig. 3.

Structural model fatigue tests were conducted by using the 2.5MN large fatigue test machine in air at room temperature, and the load was applied with sinusoidal waveform at the frequency of 0.5 to 1.0Hz. The nominal stress range,  $\Delta\sigma$ , was simply obtained in the longitudinal direction by the four point bending calculation of an I-section beam, and the stress ratio was set at 0.1. The local strain range at 5mm away from the center of a UIT line or the weld toe was measured in the longitudinal direction through strain gauges. The number of cycles to crack initiation,  $N_i$ , was defined as the fatigue life when the local strain range dropped by five percent of the initial local strain range. Fatigue crack initiation was also detected by dye penetrant testing.

### C. Plasma Arc Cut Surface Fatigue Tests

Notched plasma arc cut specimens were sampled in the plate longitudinal direction by using a CNC plasma arc cutting machine, and its condition is shown in Table 3. A plasma arc penetrated through the plate thickness, and the plasma arc moved along the outline of the specimens. Five specimens were cut out from each steel plate. Fig. 4 illustrates a notched plasma arc cut specimen used in this study. The side notch radius was 190mm, and the stress concentration factor,  $K_t$ , was 1.1.

Plasma arc cut surface fatigue tests were carried out by using a 1.0MN fatigue test machine in air at room temperature, and the load was applied with sinusoidal waveform at the frequency of 3 to 10Hz. The net section nominal stress range,  $\Delta\sigma$ , was calculated in the longitudinal direction, and the stress ratio was 0.1. The number of cycles to failure,  $N_f$ , was defined as the fatigue life.

Table 1 YP460 steel plates used for large-scale structural fatigue specimens.

Thickness (mm)	Chemical compositions (%)					Mechanical properties		
	C	Si	Mn	P	S	Yield stress (MPa)	Tensile strength (MPa)	Elongation (%)
25	0.09	0.29	1.51	0.013	0.002	564	623	20
	0.09	0.29	1.51	0.012	0.002	584	657	19
50	0.10	0.05	1.42	0.009	0.004	527	620	19

Table 2 Steel plates used for plasma arc cut surface fatigue specimens.

Steel	Thickness (mm)	Chemical compositions (%)					Mechanical properties		
		C	Si	Mn	P	S	Yield stress (MPa)	Tensile strength (MPa)	Elongation (%)
YP460	25	0.09	0.29	1.51	0.013	0.002	564	623	20
KD36	25	0.13	0.22	1.18	0.011	0.003	411	519	23

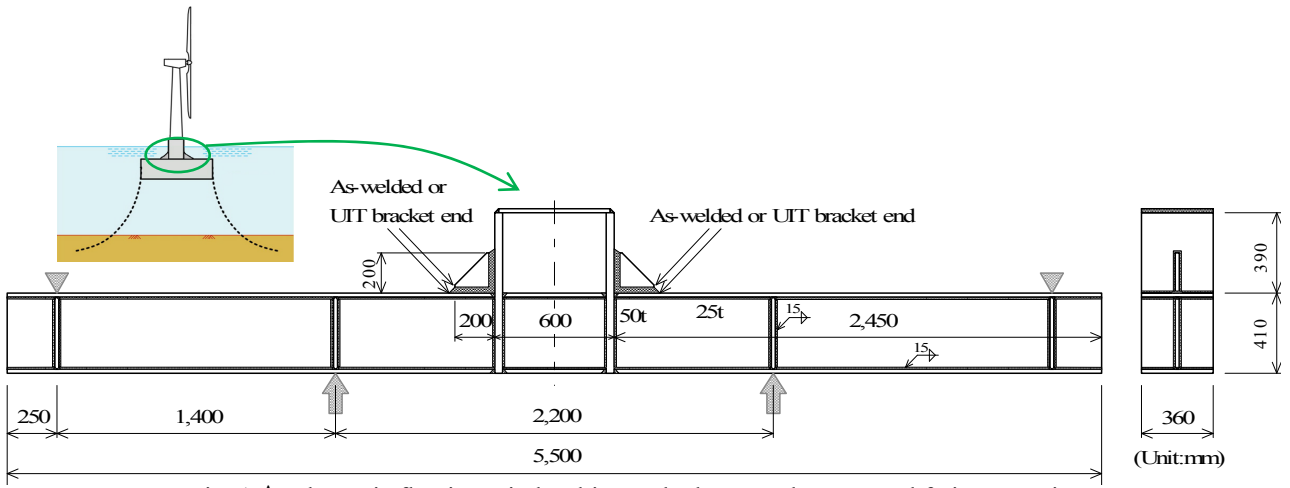


Fig. 1 A schematic floating wind turbine and a large-scale structural fatigue specimen.

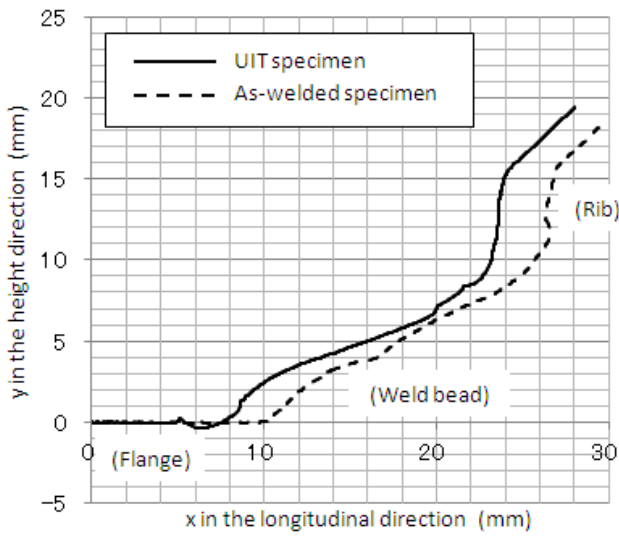


Fig. 2 Bracket end sections measured using a laser displacement sensor.

Table 3 Plasma arc cutting condition.

Machine	CNC plasma arc cutting machine
Tip bore dia.	2.5mm
Plasma gas flow rate	O <sub>2</sub> :32.5L/min
Assist gas flow rate	O <sub>2</sub> :17.5L/min, Air: 17.5L/min
Plasma current	260A
Piercing height	12.0mm
Torch height	5.0mm
Cutting speed	1350mm/min

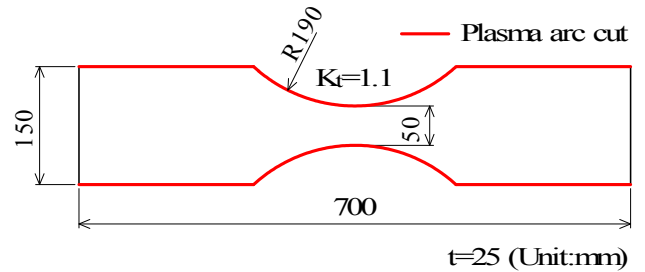


Fig. 4 Shape and size of notched plasma arc cut fatigue specimen.

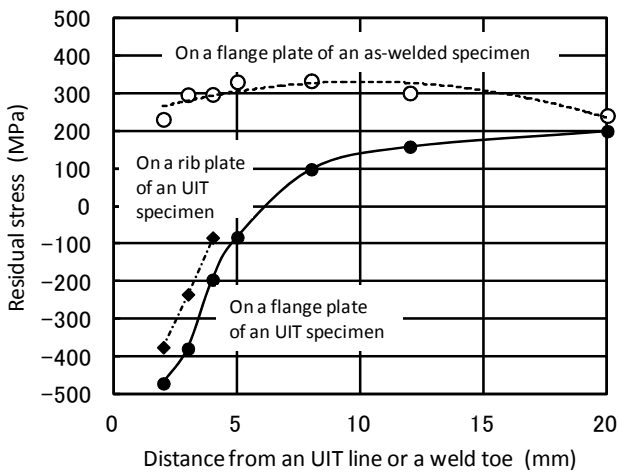


Fig. 3 Residual stress distribution.

#### D. Finite Element Analysis

Three-dimensional elastic finite element analysis was conducted using a commercial finite element analysis code,

MSC Marc 2010r2. A quarter of a large-scale structural specimen was modelled considering the symmetry conditions, as shown in Fig. 5, and the load of 1kN was applied to the inner two points of the model. Four-node isoparametric quadrilateral shell elements were used for this modeling. The structural hot spot stress,  $\sigma_{hs}$ , was determined in the vicinity of the bracket end according to the IIW fatigue design recommendations [8]. Two kinds of surface stress extrapolation methods were employed; one was fine mesh Type-a using two reference points of  $0.4t$  and  $1.0t$  ( $t$  is the plate thickness) for the weld toe on the flange plate, and the other was fine mesh Type-b using three reference points of 4mm, 8mm and 12mm for the weld toe at the rib plate edge. Meshing around the bracket ends was performed considering the surface stress extrapolation methods of IIW [8].

### III. RESULTS

#### A. Structural Model Fatigue Tests

Fig. 6 demonstrates the initial local strain changes of two structural specimens for  $\Delta\sigma=100\text{MPa}$ . Local plastic deformation around the bracket end was larger in the as-welded specimen than that in the UIT specimen, and the load versus local strain relation was almost linear in the UIT specimen.

Fig. 7 shows the relationships between  $\Delta\sigma$  and  $N_i$ , where two data points were obtained for each UIT specimen because a cracked UIT line was mended by repair welding and the other survived UIT line was re-tested in the UIT specimen. However, two or four data points were not sufficient to fit a regression S-N curve. The slope,  $m$ , of a S-N curve was accordingly determined to be the same values as those of DNV-RP-C203 [9],  $m=3$  for as-welded joints and  $m=5$  for hammer peened welded joints. The S-N curves were fitted using the following equation, where  $\log\bar{a}$  is the intercept of the  $\log N_i$ -axis by the S-N curve.

$$\log N_i = \log \bar{a} - m \cdot \log \Delta\sigma \quad (1.1)$$

All data points of UIT specimens were located in the higher fatigue strength and longer fatigue life region than as-welded specimens.

Fig. 8 shows bracket end appearances after the fatigue tests. Fatigue cracks initiated from indented surfaces at rib plate edges of the UIT specimens although fatigue cracks initiated from weld toes on flange plates of the as-welded specimens.

Analytical results were demonstrated in Fig. 9 and Fig. 10, where the maximum principal stress distributions are shown. The extrapolation of surface stress along the rib plate gave a higher structural hot stress than that on the flange plate, and the relationships between  $\Delta\sigma_{hs}$  and  $N_i$  are shown in Fig. 11, where a fatigue design S-N curve against the structural hot spot stress of bracket ends, FAT 100 in the IIW fatigue design recommendations [8], is also indicated just for reference. All data points of UIT specimens were located in the higher fatigue strength and longer fatigue life region than as-welded specimens.

#### B. Plasma Arc Cut Surface Fatigue Tests

The relationships between  $\Delta\sigma$  and  $N_i$  are shown in Fig. 12. Four of five specimens were fractured by fatigue crack growth from the notched plasma arc cut surface, and one specimen with  $s$  in the figure of each TMCP steel plate was fractured by fatigue crack growth from the original plate surface. The fatigue strength of steel base metal is proportional to the static tensile strength of the steel unless the cut surface is not deteriorated. Accordingly, S-N data of two machine cut plates, SM58Q [10] and SM50B [11], were referred to for comparison. The static strengths of SM58Q and SM50B are almost equivalent to those of YP460 and KD36, respectively. S-N data of plasma arc cut YP460 were closely located to those of machine cut SM58Q. In addition, the fatigue strength of plasma arc cut YP460 was higher than that of machine cut SM58Q in the long fatigue life region. This relation was identical in plasma arc cut KD36 and machine cut SM50B.

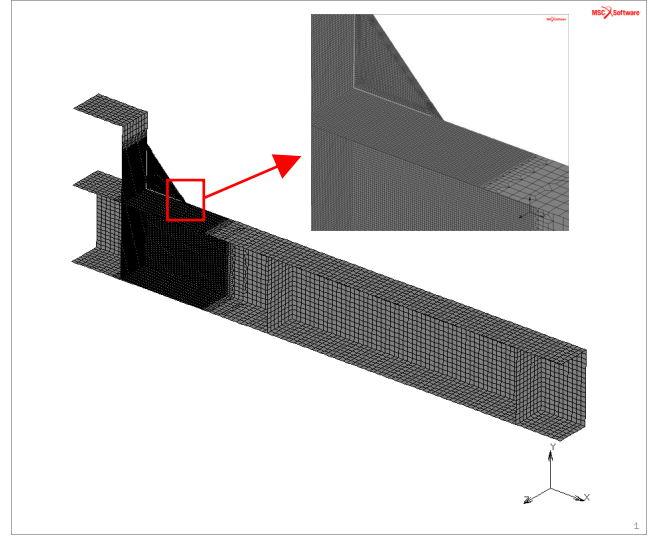


Fig. 5 Modelling and meshing of a large-scale structural fatigue specimen.

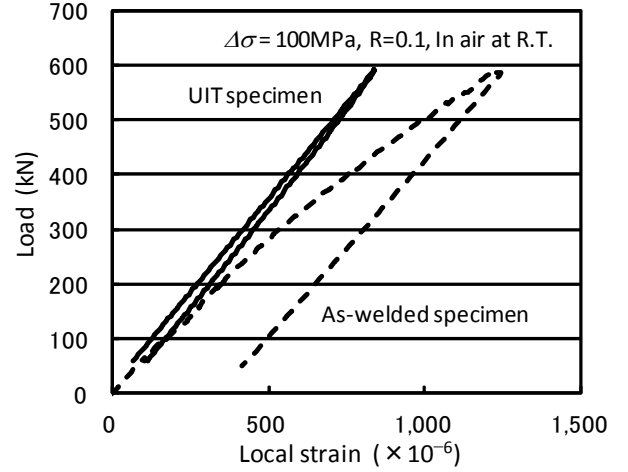


Fig. 6 Local strain changes of two large-scale structural specimens for  $\Delta\sigma=100\text{MPa}$ .

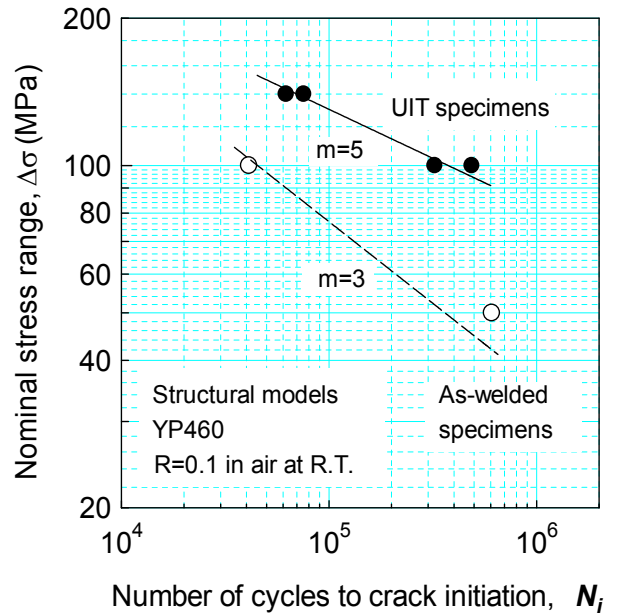
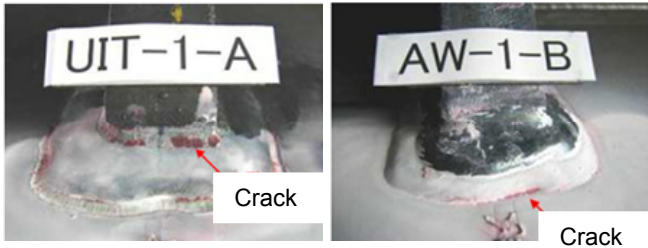


Fig. 7 Relationships between  $\Delta\sigma$  and  $N_i$  for large-scale structural specimens.



(a) UIT specimen (b) As-welded specimen

Fig. 8 Bracket end appearances after fatigue testing.

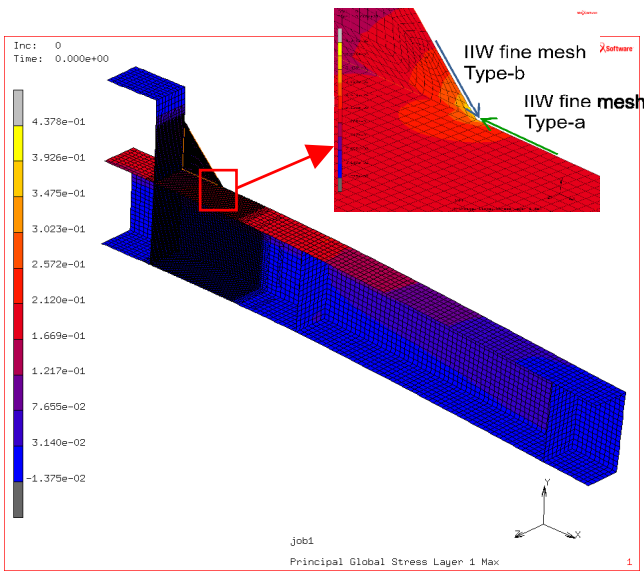


Fig. 9 Principal stress contour diagram.

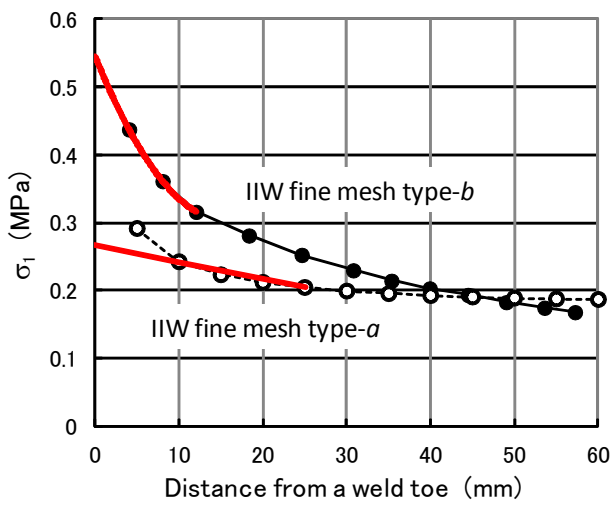
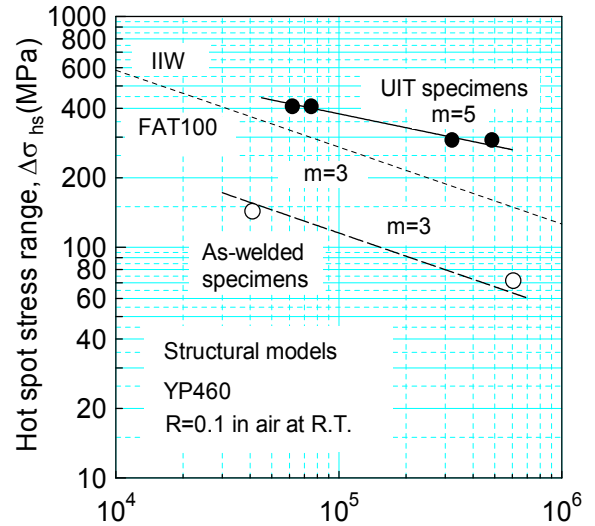
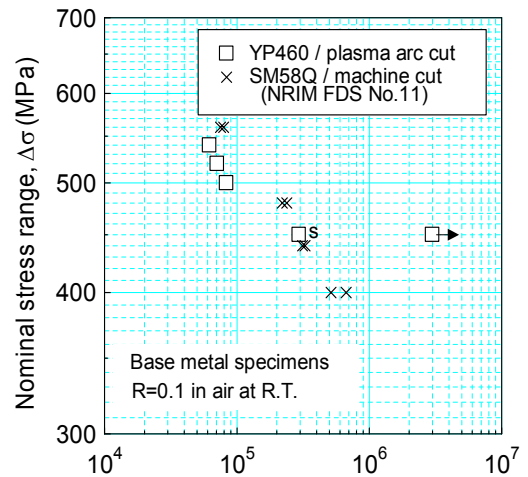


Fig. 10 Principal stress extrapolation.

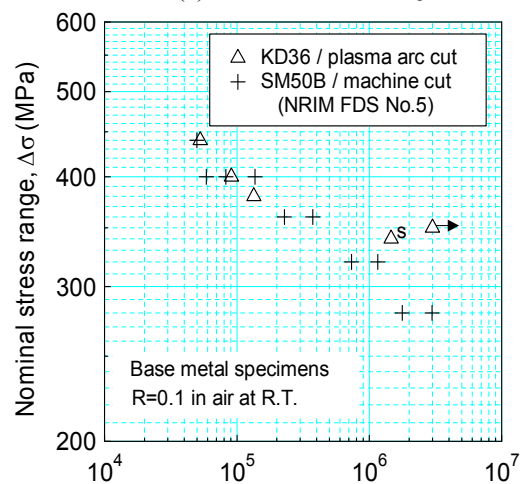


Number of cycles to crack initiation,  $N_i$

Fig. 11 Relationships between  $\Delta\sigma_{hs}$  and  $N_i$  for large-scale structural specimens.



Number of cycles to failure,  $N_f$   
(a) YP460 and SM58Q



Number of cycles to failure,  $N_f$   
(b) KD36 and SM50B

Fig. 12 Relationships between  $\Delta\sigma$  and  $N_f$  for base metal specimens.

#### IV. DISCUSSION

##### A. Effect of UIT on Fatigue Property

As shown in Fig.3, UIT induced compressive residual stress near the treated bracket end, and as shown in Fig. 6, the compressive residual stress reduced local plastic deformation near the bracket end in the low stress range region. The S-N curve of UIT specimens was consequently located in the higher fatigue strength and longer fatigue life region than that of as-welded specimens, and the effect of UIT on fatigue property improvement was particularly large in the low stress range and long fatigue life region, as demonstrated in Fig. 7. For example, the extrapolated fatigue strength of UIT specimens at  $2 \times 10^6$  cycles is twice as high as that of as-welded specimens.

The location of fatigue crack initiation changed from weld toes on flange plates in as-welded specimens to rib plate edges of UIT specimens, as shown in Fig.8. This is possibly caused by difference in residual stress and in hot spot stress.

UIT is effective in the improvement of fatigue properties as far as this study shows. However, actual loading conditions of floating wind turbine structures are potentially different from those in this study. The effect of stress ratio, average stress, preload, etc. on fatigue property improvement should be investigated for floating wind turbine structures with UIT in the future.

##### B. Steel for Plasma Arc Cutting

In each TMCP steel plate, YP460 or KD36, fatigue strength was not degraded on the plasma arc cut surface, and it was equivalent to or higher than that of the machine cut surface, as shown in Fig. 12. In addition, S-N data points of YP460 and KD36 are plotted in Fig. 13. The plasma arc cut surface of YP460 had higher fatigue strength than that of KD36. This suggests that the high strength of TMCP steel plates is advantageous to the high fatigue strength of the plasma arc cut surface even in the as-cut condition.

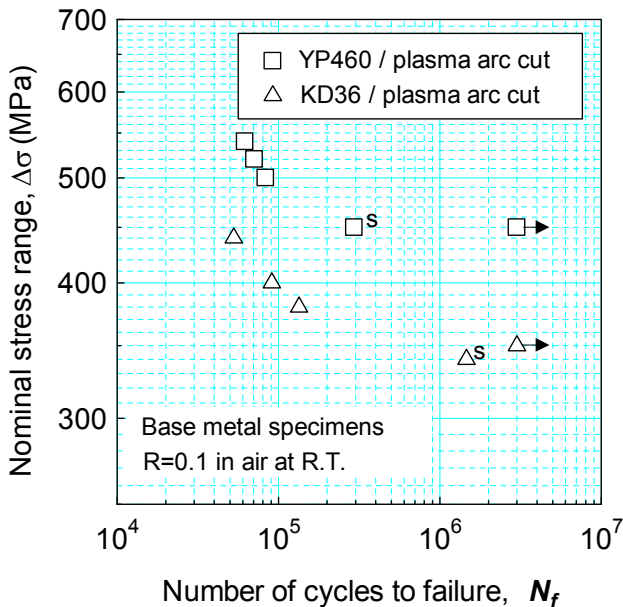


Fig. 13 S-N data points of YP460 and KD36.

#### V. CONCLUDING REMARKS

Fukushima floating offshore wind farm demonstration project has started, and two fatigue solutions, UIT and TMCP steel for plasma arc cutting, were investigated in the project.

Large-scale welded models of floating offshore wind turbine structures were manufactured using YP460 TMCP steel plates, and the bracket ends of the models were treated with UIT equipment. The effect of UIT on fatigue properties was examined by using the 2.5MN large fatigue test machine, and UIT significantly improved fatigue life particularly in the low stress range and long fatigue life region.

In addition, notched fatigue specimens were sampled by plasma arc cutting from two TMCP steel plates, YP460 and KD36, and their fatigue properties were investigated. In each TMCP steel plate, fatigue strength was not degraded on the plasma arc cut surface.

#### ACKNOWLEDGEMENTS

This study was conducted in Fukushima Floating Offshore Wind Farm Demonstration Project, and supervised by the Ministry of Economy, Trade and Industry in Japan. Useful discussions in the project are greatly acknowledged.

#### REFERENCES

- [1] T. Ishihara, "Fukushima Floating Offshore Wind Farm Demonstration Project - Current state and prospective," *J. Japan Wind Energy Association*, vol.36, No.4, pp. 553-556, 2013, (in Japanese).
- [2] E. S. Statnikov, "Comparison of post weld deformation methods for increase in fatigue strength of welded joints," *IIW Doc.*, XII-1668-97, 1997.
- [3] P. J. Haagensen, E. S. Statnikov and L. Lopez-Martinez, "Introductory fatigue tests on welded joints in high strength steel and aluminium improved by various methods including ultrasonic impact treatment (UIT)," *IIW Doc.*, XIII 1748-98, 1998.
- [4] T. Nose and H. Shimanuki, "Experiment and analysis of influence of ultrasonic peening on fatigue life in pad welded joint," *Transactions of the Japan Society of Mechanical Engineers, Series A*, vol.74, No737, pp.166-167, 2008, (in Japanese).
- [5] T. Mori, H. Shimanuki and M. Tanaka, "Effect of UIT on fatigue strength of web-gusset welded joints considering service condition of steel structures," *Welding in the world*, vol.56, pp.141-149, 2012.
- [6] T. Okawa, H. Shimanuki, Y. Funatsu, T. Nose and Y. Sumi, "Effect of preload and stress ratio on fatigue strength of welded joints improved by ultrasonic impact treatment," *Welding in the world*, vol.57, pp.235-241, 2013.
- [7] H. Yajima, Y. Kho, T. Ishikawa, M. Minagawa, K. Hirota and T. Kubo, "A study on fatigue strength in air of plasma arc cut steel plate," *Transactions of the West-Japan Society of Naval Architects*, vol.105, 2003, pp.197-204, (in Japanese).
- [8] A. Hobbacher, "Recommendations for fatigue design of welded joints and components," *WRC Bulletin 520*, IIW Doc. IIW 1823-07 ex XIII 2151r4-07/XV 1254r4-07, 2009.

- [9] Det Norske Veritas (DNV), "*Fatigue design of offshore steel structures*," DNV-RP-C203, 2011.
- [10] National Research Institute for Metals (NRIM), "*Data sheets on fatigue properties of butt welded joints of SM58Q rolled steel for welded structure – Effect of specimen size–*," NRIM fatigue data sheet No.11, 1979, (in Japanese).
- [11] National Research Institute for Metals (NRIM), "*Data sheets on fatigue properties for butt-welded joints of SM50B high tensile structural steel plates*," NRIM fatigue data sheet No.5, 1978, (in Japanese).